# Implementation of Fractional-order Model of Nickel-Cadmium Cell using Current Feedback Operational Amplifiers

Vassilis Alimisis, Marios Gourdouparis, Christos Dimas and Paul P. Sotiriadis
Department of Electrical and Computer Engineering
National Technical University of Athens, Greece
E-mail: alimisisv@gmail.com, chdim@central.ntua.gr, pps@ieee.org

***Abstract*—This work proposes an integrated-circuit architecture emulating a standard fractional-order model of Nickel-Cadmium cell for computer simulating electrochemical behavior. The architecture is based on fractional-order elements implemented with both active and passive components, offering an accurate transfer function behavior up to $250Hz$. It consists of a reduced number of active elements and implements analog all-pass filters coupled with a current conveyor. Performance and accuracy of the proposed architecture is confirmed via Monte-Carlo analysis. The proposed circuitry has been designed in TSMC $90nm$ CMOS process and simulated using the Cadence IC suite.**

***Index Terms*—Fractional calculus, fractional-order element, nickel-cadmium cell, current feedback operational amplifiers.**

## I. Introduction

Fractional calculus is a field of mathematics, suitable for modeling a variety of systems in control theory, bioengineering and electrochemistry [1]–[3]. Many researchers design integrated circuits capturing such fractional behavior which can be used in emulating real systems. To implement fractional behavior we utilize fractional-order elements. Their impedance is given by

$$Z_{element} = Z_o s^q \tag{1}$$

where $Z_o$ describes the pseudo-impedance and $q$ is the order of the element. The behavior of these elements is approximated by passive RC-networks or active components due to the fact that they are not available for massive production.

In this paper, we implement a fractional-order model of Nickel-Cadmium cell (battery), popular in electrochemistry. Electrochemistry is a branch of physical chemistry, which studies the relationship between electrical energy and chemical change [4].

Various circuits can be utilized in order to represent the cell's impedance. We choose current feedback operation amplifier (CFOA) topology for our implementation because it has excellent performance in high speed analog signal processing. Also, it provides wide bandwidth in comparison with voltage-mode circuits. In addition, it consists of current mirrors, which are used to provide bias currents (easier biasing) and current summation is available without extra components. Owing to the advantages the circuits using current feedback operation amplifiers exhibit, there are a variety of applications that can be built around these current-mode circuits [5], [6].

The remainder of the paper is organized as follows. Section II describes the fractional-order model of Nickel-Cadmium cell adopted for this design. The proposed architecture for the implementation of fractional-order capacitor is presented in Section III. The behavior of the involved model is evaluated in Section IV, in TSMC 90nm CMOS process. Finally, Section V concludes the paper.

## II. Fractional-order Nickel-Cadmium model

In this section, the fractional-order model of Nickel-Cadmium cell is presented. This model describes a type of rechargeable battery using nickel oxide hydroxide and metallic cadmium as electrodes. Except from Nickel-Cadmium cell there are several different combinations of electrode materials and electrolytes, such as Lead–Acid, Lithium-Ion and Lithium-Ion polymer cell. All these rechargeable cells have a much lower total cost of ownership, environmental impact and different types of applications [7]. Due to these characteristics, it is necessary to model the impedance of the Nickel-Cadmium cell.

The electrical analogue of the electrochemical model, which introduced in [3], [8] is depicted in Fig. 1. It is constructed from two resistors and two fractional-order capacitors which act as Constant Phase Elements (CPEs), with pseudo-capacitance expressed in $\mathrm{Farad/sec}^{1-\alpha}$ (where $\alpha$ is the order of the element). The total impedance of the fractional-order model is given by:

$$Z_{model}(s) = R_o + \frac{R_1 C_2 s^{a_1+a_2} + 1}{C_1 C_2 R_1 s^{a_1+a_2} + C_1 s^{a_1} + C_2 s^{a_2}} \tag{2}$$

where $R_o$ and $R_1$ are the resistors of the model. Also, $C_1$ is the pseudo-capacitance and $a_1$ is the order of the first fractional-order capacitor (double layer element) and $C_2$ is the pseudo-capacitance and $a_2$ is the order of the second fractional-order capacitor (Warburg element) [3]. The frequency range of practical interest is set to be from $2mHz$ to $250Hz$ for the corresponding model and model's parameters, as estimated in [3], [8] are summarized in Table I.

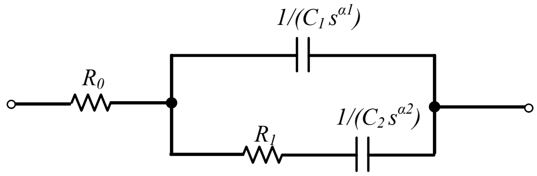


Fig. 1. Fractional-order model of Nickel-Cadmium cell.

TABLE I
COMPONENT VALUES OF THE CIRCUIT IN FIG. 1.

| Element | Value | Element | Value |
|---|---|---|---|
| $R_o$ | $6.68\,\mathrm{k\Omega}$ | $C_1$ | $0.79\,\mu\mathrm{F/sec}^{0.24}$ |
| $R_1$ | $2.72\,\mathrm{k\Omega}$ | $C_2$ | $0.16\,\mu\mathrm{F/sec}^{0.37}$ |

## III. Proposed Circuit Architecture

Since fractional-order capacitors are not yet available for massive production, the behavior of the fractional-order model of Nickel-Cadmium cell is approximated by active and passive elements. In this section, we present an architecture for the implementation of fractional-order capacitors. Owing to the fact that the frequency span is from $2mHz$ to $250Hz$ the employment of the $5^{th}$-order Continued Fraction Expansion (CFE) approximation is a necessary solution, but it is not the optimal (very complex design) [9]–[12].

In this case, the behavior of fractional-order capacitor is described by utilizing Current Feedback Operational Amplifiers (CFOAs) and Current Conveyors (CCII) as active elements and our architecture is based on the reduction of their number, compared to other implementations. In order to achieve this, we separate the frequency range in two domains. This reduces the order of CFE and the complexity of the proposed design. The frequency range is set to be from $2mHz$ to $700mHz$ for Case I and from $700mHz$ to $250Hz$ for Case II and we choose $3^{rd}$-order CFE approximation round a center frequency $\omega_o = 1/\tau$ [9]–[12]. The expression of the $3_{rd}$-order CFE approximation is described by

$$(\tau s)^{\alpha} \approx \frac{a_3 s^3 + a_2 s^2 + a_1 s + a_o}{b_3 s^3 + b_2 s^2 + b_1 s + b_o} \tag{3}$$

where:
$\alpha_3 = b_o = \alpha^3 + 6\alpha^2 + 11\alpha + 6,$
$\alpha_2 = b_1 = -3\alpha^3 - 6\alpha^2 + 27\alpha + 54,$
$\alpha_1 = b_2 = 3\alpha^3 - 6\alpha^2 - 27\alpha + 54,$
$\alpha_o = b_3 = -\alpha^3 + 6\alpha^2 - 11\alpha + 6$
and $\alpha$ is the order of the differentiator [9]–[12].

Fractional-order capacitors are implemented by a fractional-order differentiator in a connection with a double-output Current Conveyor (DO-CCII) acting as Voltage to Current (V/I) converter. The complete design is depicted in Fig. 2 and parameters are summarized in Table II. The implementation of the fractional-order differentiator is based on a $3_{rd}$-order all pass filter and the transfer function is given by

$$H(s) = (\tau s)^{\alpha} = \frac{a_3 s^3 + a_2 s^2 + a_1 s + a_o}{b_3 s^3 + b_2 s^2 + b_1 s + b_o} \tag{4}$$

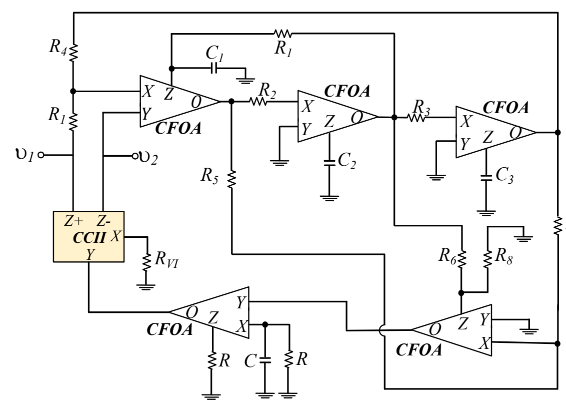


Fig. 2. Implementation of fractional-order capacitor emulator.

The impedance of the fractional-order capacitor is given by:

$$Y_{cap}(s) = \frac{R_{vi}}{H(s)} \tag{5}$$

where $R_{vi}$ is the appropriate resistor of the V/I converter and $H(s)$ is the expression of the filter.

TABLE II
PARAMETER OF THE CIRCUIT IN FIG. 2.

| Parameter | Value | Parameter | Value |
|---|---|---|---|
| $b_3$ | $1$ | $b_2$ | $\frac{1}{R_1 C_1}$ |
| $b_1$ | $\frac{b_2}{R_2 C_2}$ | $b_o$ | $\frac{b_1}{R_3 C_3}$ |
| $\alpha_3$ | $\frac{b_2 R_6 R_8 RC}{R_5(R_6+R_8)}$ | $\alpha_2$ | $\frac{\alpha_3}{RC} + \frac{b_1 R_8 RC}{R_5(R_6+R_8)}$ |
| $\alpha_o$ | $\frac{b_o R_6 R_8}{R_7(R_6+R_8)}$ | $\alpha_1$ | $RC\alpha_o + \frac{b_1 R_8}{R_6+R_8}$ |

## IV. Simulation Results

The proposed Nickel-Cadmium cell has been designed in TSMC $90\,\mathrm{nm}$ CMOS process, using the Cadence IC design suite. The schematic of the corresponding CFOA is depicted in Fig. 3 and the schematic of the appropriate V/I converter is shown in Fig. 4. The power supply rails are set to $V_{DD} = -V_{SS} = 0.75\,\mathrm{V}$, $I_b = 200nA$, $I_{bias} = 1nA$ and all transistors operate in the sub-threshold region. The dimensions of the MOS transistors of the CFOA and the DO-CCII are summarized in Table III.

TABLE III
MOS TRANSISTORS DIMENSIONS – CFOA & DO-CCII.

| CFOA | W/L (μm/μm) | DO-CCII | W/L (μm/μm) |
|---|---|---|---|
| $M_{n1}$-$M_{n9}$ | 13/0.5 | $M_{n1}$-$M_{n9}$ | 13/0.5 |
| $M_{p5}$-$M_{p10}$ | 50/0.5 | $M_{p4}$-$M_{p10}$ | 50/0.5 |
| $M_{p11}$,$M_{p12}$ | 100/0.5 | $M_{p3}$ | 100/0.5 |
| $M_{p1}$-$M_{p4}$ | 20/0.4 | $M_{p1}$,$M_{p2}$ | 20/0.4 |

The values of the passive elements of Fig. 2 for the approximation of fractional-order capacitors are summarized

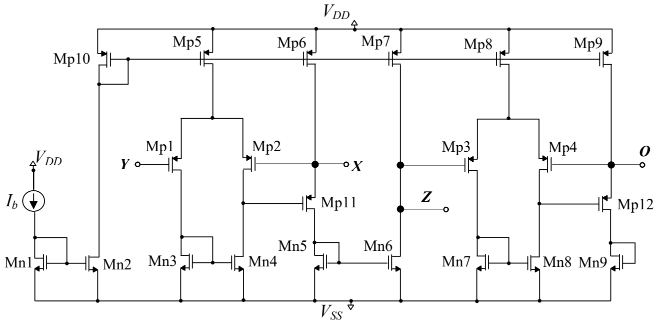


Fig. 3. Employed CFOA.

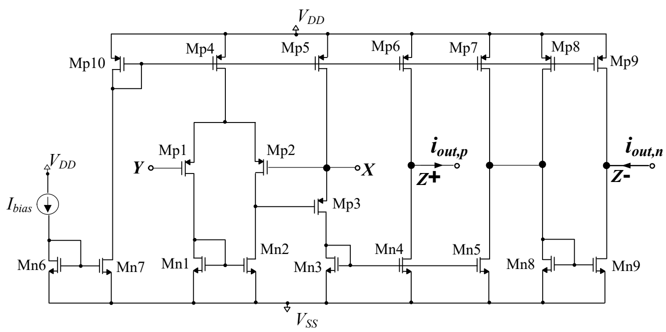


Fig. 4. Employed DO-CCII for the implementation of V/I converter.

TABLE IV
PASSIVE ELEMENTS' VALUES FOR APPROXIMATING THE FRACTIONAL-ORDER CAPACITOR $C_1$ WITH ORDER $\alpha_1 = 0.76$.

| Case I Element | Value | Case II Element | Value |
|---|---|---|---|
| $C_1$ | 467.0 nF | $C_1$ | 750.0 pF |
| $C_2$ | 17.40 $\mu$F | $C_2$ | 47.67 nF |
| $C_3$ | 330.0 $\mu$F | $C_3$ | 850.0 nF |
| $C$ | 9.21 $\mu$F | $C$ | 23.50 nF |
| $R_1$ | 100.0 k$\Omega$ | $R_1$ | 100.0 k$\Omega$ |
| $R_2$ | 100.0 k$\Omega$ | $R_2$ | 100.0 k$\Omega$ |
| $R_3$ | 105.0 k$\Omega$ | $R_3$ | 85.0 k$\Omega$ |
| $R_4$ | 100.0 k$\Omega$ | $R_4$ | 100.0 k$\Omega$ |
| $R_5$ | 126.9 k$\Omega$ | $R_5$ | 120.0 k$\Omega$ |
| $R_6$ | 85.0 k$\Omega$ | $R_6$ | 85.0 k$\Omega$ |
| $R_7$ | 4.0 M$\Omega$ | $R_7$ | 4.0 M$\Omega$ |
| $R_8$ | 103.8 k$\Omega$ | $R_8$ | 68.40 k$\Omega$ |
| $R$ | 1.0 M$\Omega$ | $R$ | 1.20 M$\Omega$ |
| $R_{VI}$ | 200.0 k$\Omega$ | $R_{VI}$ | 120.0 k$\Omega$ |

in Table IV for capacitor $C_1$ with order $\alpha_1$ and in Table V for capacitor $C_2$ with order $\alpha_2$.

The obtained magnitude and phase responses in comparison with both approximation and theoretically predicted ones confirm the behavior of the fractional-order capacitors $C_1, \alpha_1$ and $C_2, \alpha_2$ for both cases as shown in Fig. 5 and Fig. 6. Theoretical and approximation responses are the same for the case of the impedance. The results of the proposed impedance models are in fine agreement with the approximation ones as it is depicted in Fig. 7 and Fig. 8. The Mean Absolute Error (MAE) between the simulation and the approximation for model is less than $42.11k\Omega$ for impedance and $0.51°$ for phase for Case I and less than $5.52k\Omega$ for impedance and $1.33°$ for phase for Case II. The obtained simulation results confirm the proper operation, performance and accuracy of the proposed topology.

The sensitivity behavior has been evaluated using the Monte-Carlo analysis tool for $N = 100$ runs. It is a broad class of computational algorithms that rely on repeated random sampling to obtain circuit parameters. The corresponding histograms for impedance and phase for Case II are demonstrated in Fig. 9, respectively. The mean value of the impedance and phase is $I_{mean} = 46.83\,\text{k}\Omega$ and $P_{mean} = -60.78°$ and the standard deviation is $\sigma_I = 1.38\,\text{k}\Omega$ and $\sigma_P = 1.21°$ at $f_o = 10\,\text{Hz}$, respectively. The Monte-Carlo analysis demonstrates the performance and accuracy of the proposed architecture. Finally, the number of components in comparison with previous work are summarized in Table VI.

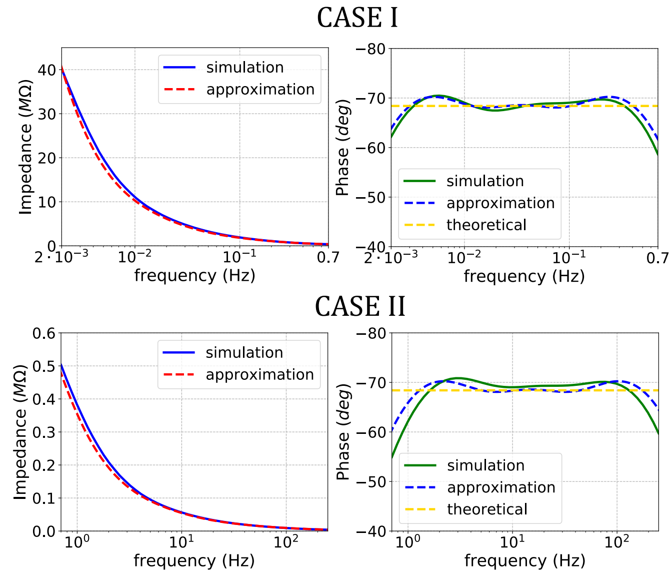


Fig. 5. Frequency responses of fractional-order capacitor $C_1$ with order $\alpha_1$.

TABLE V
PASSIVE ELEMENTS' VALUES FOR APPROXIMATING THE FRACTIONAL-ORDER CAPACITOR $C_2$ WITH ORDER $\alpha_2 = 0.63$.

| Case I Element | Value | Case II Element | Value |
|---|---|---|---|
| $C_1$ | 440.0 nF | $C_1$ | 2.10 nF |
| $C_2$ | 18.69 $\mu$F | $C_2$ | 45.30 nF |
| $C_3$ | 438.26 $\mu$F | $C_3$ | 1.07 $\mu$F |
| $C$ | 12.57 $\mu$F | $C$ | 33.0 nF |
| $R_1$ | 100.0 k$\Omega$ | $R_1$ | 80.0 k$\Omega$ |
| $R_2$ | 100.0 k$\Omega$ | $R_2$ | 150.0 k$\Omega$ |
| $R_3$ | 100.0 k$\Omega$ | $R_3$ | 140.0 k$\Omega$ |
| $R_4$ | 100.0 k$\Omega$ | $R_4$ | 80.0 k$\Omega$ |
| $R_5$ | 219.2 k$\Omega$ | $R_5$ | 140.0 k$\Omega$ |
| $R_6$ | 90.0 k$\Omega$ | $R_6$ | 65.0 k$\Omega$ |
| $R_7$ | 1.2 M$\Omega$ | $R_7$ | 3.0 M$\Omega$ |
| $R_8$ | 95.7 k$\Omega$ | $R_8$ | 150.0 k$\Omega$ |
| $R$ | 700.0 k$\Omega$ | $R$ | 900.0 k$\Omega$ |
| $R_{VI}$ | 800.0 k$\Omega$ | $R_{VI}$ | 4.0 M$\Omega$ |

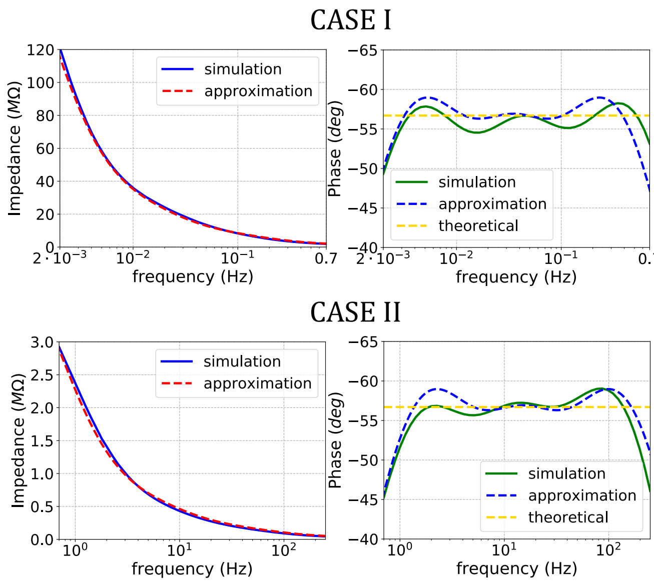


Fig. 6. Frequency responses of fractional-order capacitor $C_2$ with order $\alpha_2$.

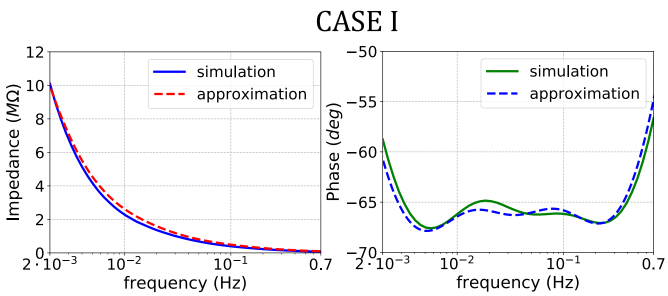


Fig. 7. Frequency responses of fractional-order model of Nickel-Cadmium cell-Case I.

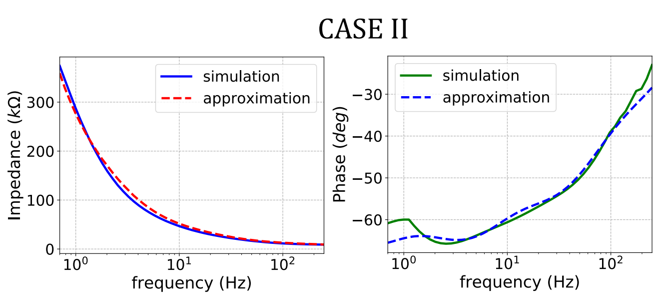


Fig. 8. Frequency responses of fractional-order model of Nickel-Cadmium cell-Case II.

TABLE VI
COMPONENTS SUMMARY.

| | V/I | CFOAs | Resistors | Capacitors | CFE approx. |
|---|---|---|---|---|---|
| This work | 1 | 5 | 11 | 4 | $3^{rd}-order$ |
| [12] | 1 | 5 | 10 | 2 | $2^{nd}-order$ |

## V. CONCLUSION

In this paper, we implemented the Nickel-Cadmium cell in fractional order integrated form using CFOAs and CCIIs as active elements. Simulations showed very low impedance and phase errors for fractional-order capacitors, while model's simulations confirm the accuracy and the performance of the proposed architecture, in system level. The circuit implemented can be used as a basic building block for the design of more complex and accurate systems.

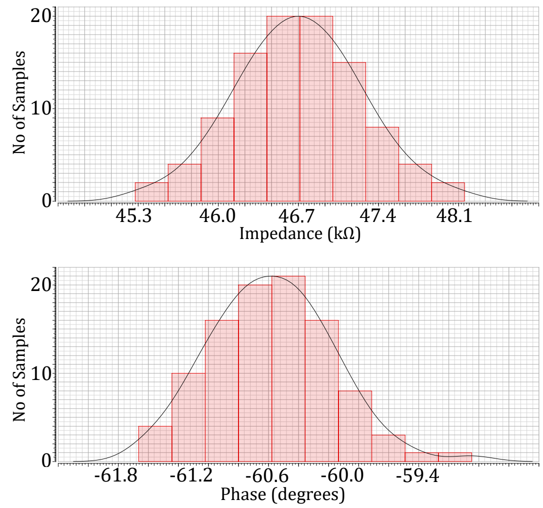


Fig. 9. Sensitivity performance of impedance (upper) and phase (down) using Monte-Carlo analysis.

## REFERENCES


[1] C. A. Monje, Y. Chen, B. M. Vinagre, D. Xue, and V. Feliu-Batlle, *Fractional-order systems and controls: fundamentals and applications*. Springer Science & Business Media, 2010.

[2] R. L. Magin, *Fractional calculus in bioengineering*. Begell House Redding, 2006, vol. 2, no. 6.

[3] T. J. Freeborn, B. Maundy, and A. S. Elwakil, "Fractional-order models of supercapacitors, batteries and fuel cells: a survey," *Materials for Renewable and Sustainable Energy*, vol. 4, no. 3, p. 9, 2015.

[4] V. S. Bagotsky, *Fundamentals of electrochemistry*. John Wiley & Sons, 2005, vol. 44.

[5] C. Toumazou, J. Lidgey, and A. Payne, "Emerging techniques for high frequency bjt amplifier design: a current mode perspective," in *Proceedings of the 1st International conference on Electronics, Circuits and Systems*, 1994, pp. 56–57.

[6] A. M. Soliman, "Applications of the current feedback operational amplifiers," *Analog Integrated Circuits and Signal Processing*, vol. 11, no. 3, pp. 265–302, 1996.

[7] W. Jiang and B. Fahimi, "Active current sharing and source management in fuel cell–battery hybrid power system," *IEEE Transactions on Industrial Electronics*, vol. 57, no. 2, pp. 752–761, 2009.

[8] V. Viswanathan, A. Salkind, J. Kelley, and J. Ockerman, "Effect of state of charge on impedance spectrum of sealed cells part i: Ni-cd cells," *Journal of applied electrochemistry*, vol. 25, no. 8, pp. 716–728, 1995.

[9] G. Tsirimokou, C. Psychalinos, and A. Elwakil, *Design of CMOS analog integrated fractional-order circuits: applications in medicine and biology*. Springer, 2017.

[10] V. Alimisis, P. Bertsias, C. Psychalinos, and A. S. Elwakil, "Electronically tunable implementation of the arterial viscoelasticity model," in *2019 42nd International Conference on Telecommunications and Signal Processing (TSP)*. IEEE, 2019, pp. 145–148.

[11] C. Vastarouchas, C. Psychalinos, and A. S. Elwakil, "Fractional-order model of a commercial ear simulator," in *2018 IEEE International Symposium on Circuits and Systems (ISCAS)*. IEEE, 2018, pp. 1–4.

[12] I. Dimeas, G. Tsirimokou, C. Psychalinos, and A. S. Elwakil, "Realization of fractional-order capacitor and inductor emulators using current feedback operational amplifiers," *a a*, vol. 2, no. 8, p. 2, 2015.